Interfacial Enhancement of Maleated Polypropylene/Silica Composites Using Graphene Oxide

Feng Luo, Li Chen, Nanying Ning, Ke Wang, Feng Chen, Qiang Fu

Department of Polymer Science and Materials, State Key Laboratory of Polymer Materials Engineering, Sichuan University, Chengdu 610065, People's Republic of China

Received 7 July 2011; accepted 7 October 2011
DOI 10.1002/app.36224
Published online 17 January 2012 in Wiley Online Library (wileyonlinelibrary.com).

ABSTRACT: Graphene oxide (GO) is derived from oxidization of natural graphite and contains many active groups. These active groups make GO a potential compatibilizer for polymer blends or coupling agent for polymer composites. In this work, a novel core-shell structured hybrid submicroparticles of graphene oxide-encapsulated silica (GO-SiO_2) were fabricated using GO sheets via an electrostatic assembly between ultrathin negatively charged graphene oxide sheets and positively charged amino-modified silica. The possible application of this new hybrid filler was explored in preparation of maleated polypropylene (PP-*g*-MA)/GO-SiO_2 composites. The microstructure and interface enhancement of the prepared composites were analyzed by SEM, TEM, OM, TGA, FTIR, and DMA measurements. A uniform dispersion of GO-SiO_2 hybrids, enhanced interfacial adhesion and improved mechanical property were evidenced. The reason might be that graphene oxide can be covalently assembled onto the amino-modified silica surface, and simultaneously it provides strong interaction with the PP-*g*-MA due to similar polarity or possible hydrogen bonding. This work suggests a potential application of graphene oxide-encapsulated particle in preparation of high performance polymer composites. © 2012 Wiley Periodicals, Inc. J Appl Polym Sci 125: E348–E357, 2012

Key words: graphene oxide; silica; interfacial enhancement; core-shell structure; polypropylene

INTRODUCTION

Graphene is a two-dimensional (2D) sheet carbon material consisting of planar monolayered hexagonal sp2 hybridized carbons.[1,2] Recently, it has attracted both academic and industrial interest because it can produce a dramatic improvement in properties of polymer/graphene composites at very low filler content due to its unique properties such as high mechanical properties,[3] electronic[4] and thermal conductivity,[5] mobility of charge carriers,[6] and specific surface area.[7] Since it was first achieved in 2004 using micromechanical cleavage from graphite,[8] various effective techniques such as chemical vapor deposition,[9] epitaxial growth,[10,11] mechanical,[8] or chemical exfoliations,[12,13] have been developed to produce graphene. Among those, oxidative exfoliation of naturally abundant graphite and subsequent reduction may offer a highly efficient route to produce chemically functionalized graphene.[14–16]

Graphene oxide (GO) is derived from the oxidization of natural graphite flakes followed by ultrasonic treatment of the suspension. In contrast to pristine graphite, the graphene oxide sheets are heavily oxygenated, whose basal planes are decorated mostly with epoxide, hydroxyl, carbonyl, and carboxyl groups.[17,18] These active groups make GO as a potential compatibilizer for polymer blends or coupling agent for polymer composites. On the basis of the superior natures of graphene oxide (graphene), several core-shell hybrid particles and their applications have been developed. Yang et al.[19] described a novel strategy for the fabrication of graphene-encapsulated metal oxide by electrostatic forces into core-shell hybrids. This hybrid structure enabled a good encapsulation of electrochemically active metal oxide nanoparticles by graphene sheets, thus leading to remarkable lithium-storage performance. Han et al.[20] introduced a straightforward hybrid assembly of graphene and biomolecules into core/shell nanowires. A supercapacitor electrode with highly entangled networks of the hollow graphene shell has been achieved. Luechinger et al.[21] showed a mechanical wrapping of an inorganic particle with graphene sheets and made them amenable to polymer dispersion (even at metal loadings of up to 90 wt %). Hollow multilayer capsules and porous paper of graphene oxide nanosheets were also skillfully prepared by using graphene oxide (GO) sheets

Correspondence to: K. Wang (wkestar@scu.edu.cn) or Q. Fu (qiangfu@scu.edu.cn).

Contract grant sponsor: National Natural Science Foundation of China; contract grant numbers: 50903048, 21034005.

wrapped on polymer microspheres.[22,23] Moreover, a series of metal (metal oxide) particles including gold,[24] silver,[25] platinum,[26] zinc oxide,[27] titanium dioxide,[28] etc. have been introduced onto the surface of GO, giving rise to novel nanohybrids with improved performance.

In this work, we described a novel strategy for the fabrication of core-shell GO-SiO_2 hybrid particles by coassembly between negatively charged graphene oxides and positively charged amino-modified silica particles. Silica is a very important material which has been employed in a variety of applications in current industry.[29] With the ultrathin GO sheets coated on silica surface, its surface structure and chemical properties are subsequently changed, which endows it with potential specific application. To demonstrate the applications of this new hybrid filler, it was added into the maleated polypropylene by melt blending. A uniform dispersion and strong interfacial interaction were observed, resulting in an obviously improved mechanical property. It is anticipated that these GO–SiO_2 hybrid particles may find broad potential application in the preparation of functionalized and reinforced polymer composites.

EXPERIMENTAL

Materials

Graphite powders were purchased from Qingdao Black Dragon graphite. Submicro sized silica (median size = 500 nm) was purchased from Admatechs. Potassium permanganate ($KMnO_4$), sulfuric acid (H_2SO_4 98%), sodium nitrate ($NaNO_3$), and hydrogen peroxide (H_2O_2) were purchased from Kermel Chemical reagent plant (Chengdu, China), all reagents were used as received. 3-aminopropyltriethoxysilane (APS) was provided from commercial sources, and used without purification. A maleated polypropylene (PP-*g*-MA) with maleic anhydride content = 0.9 wt %, $M_w = 21.1 \times 10^4$ g/mol, and $M_w/M_n = 3.2$ (Chenguang Technology Chengdu, China) was used as the base polymer.

Fabrication of graphene oxide-encapsulated silica hybrids

Surface modification of SiO_2 with APS coupling agent was performed by the following procedure: Briefly, SiO_2 powder (10 g), was mixed with 0.5 mL APS and 2 mL deionized water in 150 mL ethanol by planetary ball mill with zirconia balls (400 rpm, 30 min) to get well-dispersed SiO_2 suspension. Then, the mixture was stirred and heated up to 60°C for 24 h to realize grafting reaction completely. After reaction, the particles were filtered from the mixture, then washed with ethanol and deionized water five times to remove unreacted coupling agent.

GO was obtained by using Hummers method,[30] followed by ultrasonication for 90 min to produce well-dispersed graphene oxide sheets. The nonexfoliated GO sheets were removed by centrifuged (3000 rpm). Then the GO colloid solution was diluted to a concentration of 0.15 mg/mL with additional deionized water.

GO encapsulated silica hybrids (GO-SiO_2) were fabricated simply by mixing the aqueous suspension of positively charged amino-modified SiO_2 (SiO_2-NH_3^+) particles and negatively charged GO sheets. Under optimal conditions, almost all GO sheets precipitated with SiO_2-NH_3^+ where the coated GO shell was about 1 wt % of the SiO_2 particles. In a typical process, 300 mL SiO_2-NH_3^+ suspension (25 mg/mL) was slowly added into a 500-mL aqueous GO suspension (0.15 mg/mL) under mild magnetic stirring for 2 h. The obtained GO-SiO_2 hybrids were centrifuged and washed with deionized water, then dried in a vacuum oven at 60°C for 24 h before use.

Preparation of maleated polypropylene composites

Melt blending of PP-*g*-MA with a weight percentage of 1, 3, 5, and 10% of GO-SiO_2 powders was conducted using a mixer (HAAKE, RS600, Germany) at a temperature of 200°C for 5 min and the screw speed was 50 rpm. After making pieces and dried under vacuum at 60°C for 2 h, the as-prepared samples were injection-molded into tensile testing bars with dimensions of 75 × 4.0 × 2.0 mm^3 (length × wide×thickness) using a mini-injection system (Thermo Scientific, USA) at melt temperature of 210°C and mold temperature of 30°C. For comparison, the neat PP-*g*-MA and samples with same weight percentage of pristine SiO_2 and amino-modified SiO_2 were also prepared by the identical procedure. In a convenient manner, the weight loading of filler was directly labeled in front of composites. For example, 10% PP-*g*-MA/GO-SiO_2 means PP-*g*-MA with 10 wt % GO-SiO_2 hybrids.

To investigate the interactions between PP-*g*-MA and GO-SiO_2 (SiO_2) surface, the composites were extracted in boiling xylene for 4 h by Soxhlet extraction technique. The extracted fillers was washed with ethanol for five times, and then dried in a vacuum oven at 60°C for 24 h before measurement. The extracted fillers from PP-*g*-MA/GO-SiO_2 and PP-*g*-MA/SiO_2 are designated as Ex-GO-SiO_2 and Ex-SiO_2, respectively.

Characterization

FTIR was employed to characterize chemical structure of SiO_2, Ex-SiO_2, and Ex-GO-SiO_2. The spectra

were recorded between 400 and 4000 cm^{-1} on a Nicolet-560 infrared spectrometer. Zeta potential measurements were performed using a Zetasizer 3000 (Malvern Instruments, UK), and the GO and silica samples were diluted to 0.05, 2 mg/mL, respectively, before measurements.

Transmission electron microscopy (TEM) observations were carried out to examine the micro-morphology of hybrids on a Tecnai F20 S-TWIN TEM under an acceleration voltage of 200 kV. The scanning electron microscopy (SEM) experiments were performed using a FEI Inspect F scanning electron microscopy (SEM) instrument with an acceleration voltage of 20 kV. The microscopic morphology of hybrid particles and cryogenically fractured surfaces of composites were observed. The dispersions of particles in the matrix via melt blending were collected by the Leica DMIP optical microscopy (OM).

The thermal stability was studied by Thermal gravimetric analysis (TGA) test, conducted at Q500 Thermogravimetric analyzer (TA instruments, USA) from 30 to 550°C at nitrogen atmosphere with the heating of 10°C/min.

Dynamic mechanical analysis (DMA) tests of neat PP-*g*-MA and composites were carried out using a DMA Q800 analyzer (TA instruments, USA) to determine their thermomechanical properties. The three-point-bend mode was used, and the measurement was carried out on a rectangular shaped part in the size of 30 × 4.0 × 2.0 mm^3 (length × wide × thickness) from −50 to 100°C at a heating rate of 3°C/min and an oscillatory frequency of 1 Hz.

Standard tensile tests were performed on a dumbbell-shaped specimen using an SANS Universal tensile testing machine according to the ASTM D638-03 standard with a crosshead speed of 50 mm/min. Five samples were used for each measurement and the average result was reported.

RESULTS AND DISCUSSION

Self-assembly and morphology of graphene oxide-encapsulated silica

Recent studies showed that GO sheets could be regarded as two-dimensional conjugated macromolecules with huge molar masses, and the unique molecule-colloid duality GO sheets were proved repeatedly as an ideal 2D building block by assembling into macroscopic materials with hierarchical structures via certain interactions.[17,31,32] Originating from ionization of the carboxylic acid and phenolic hydroxy groups introduced by chemical oxidation on the sheets surface, GO exhibited high negatively charged surface. Thanks to its negatively charged surface, GO could coassemble with some positively charged materials via mutual electrostatic interaction.[20,33]

Here, the SiO_2 was firstly modified by APS, which could be ionization of amino groups to form positively charged SiO_2-NH_3^+ particles.[22] Therefore, it is easy to assume that electrostatic driving force can take place between these two materials. To clarify this process, zeta potential tests were taken to examine the surface charges of GO, SiO_2, and amino-modified SiO_2 aqueous suspensions. With pH value 7, the GO had a high negatively charged surface with ζ potential value of −39.6 mV. Apparently, this charge originated from the ionization of the carboxylic acid and phenolic hydroxy groups that were located on the graphene oxide.[34] Meanwhile, the surface charges of the silica switched from negative (ζ potential = −25.6 mV) to positive (ζ potential = 42.2 mV) after APS modification. For amino-modified SiO_2 particle, the grafting and the protonating effect of amino group on its surface made its surface positively charged in aqueous media. When the oppositely charged GO sheets and SiO_2-NH_3^+ particles met through a simple solution mixing, the electrostatic assembly might be triggered, forming the core-shell structure of GO-SiO_2 hybrids afterward.

The morphology and microstructure of the GO-SiO_2 hybrids and the pristine SiO_2 are shown in Figure 1. Macroscopically, the hybrid particles show dark gray color in contrast with the white color that pristine SiO_2 particles show [Fig. 1(a)], indicating that the surface of the SiO_2 particles were coated uniformly with GO sheets. Microcosmically, the GO-SiO_2 hybrids showed crinkled and rough textures that were associated with the presence of flexible and ultrathin graphene oxide sheets. In most cases, the edges of individual as well as overlapping GO layers could be observed, particularly at the interface between aggregated particles, where the GO layers appeared to link neighboring particles together [Fig. 1(c)]. In contrast, SEM images of uncoated SiO_2 particles showed only smooth unfeatured surfaces [Fig. 1(b)]. Close inspection of the fine features of the GO-SiO_2 hybrids by TEM confirmed the extremely thin (<5 nm), flexible, and corrugated nature of the GO shells [Fig. 1(d)]. This result suggests an intimate encapsulation of the silica particles by GO sheets. Therefore, the novel core-shell structured GO-SiO_2 hybrids were fabricated by electrostatic attraction through a simple solution mixing.

Dispersion of core-shell structured GO-SiO_2 hybrids in maleated polypropylene composites

To explore the properties and applications of these novel hybrids, the hybrids were added to maleated polypropylene (PP-*g*-MA). The composites were simply prepared via melt compounding of maleated

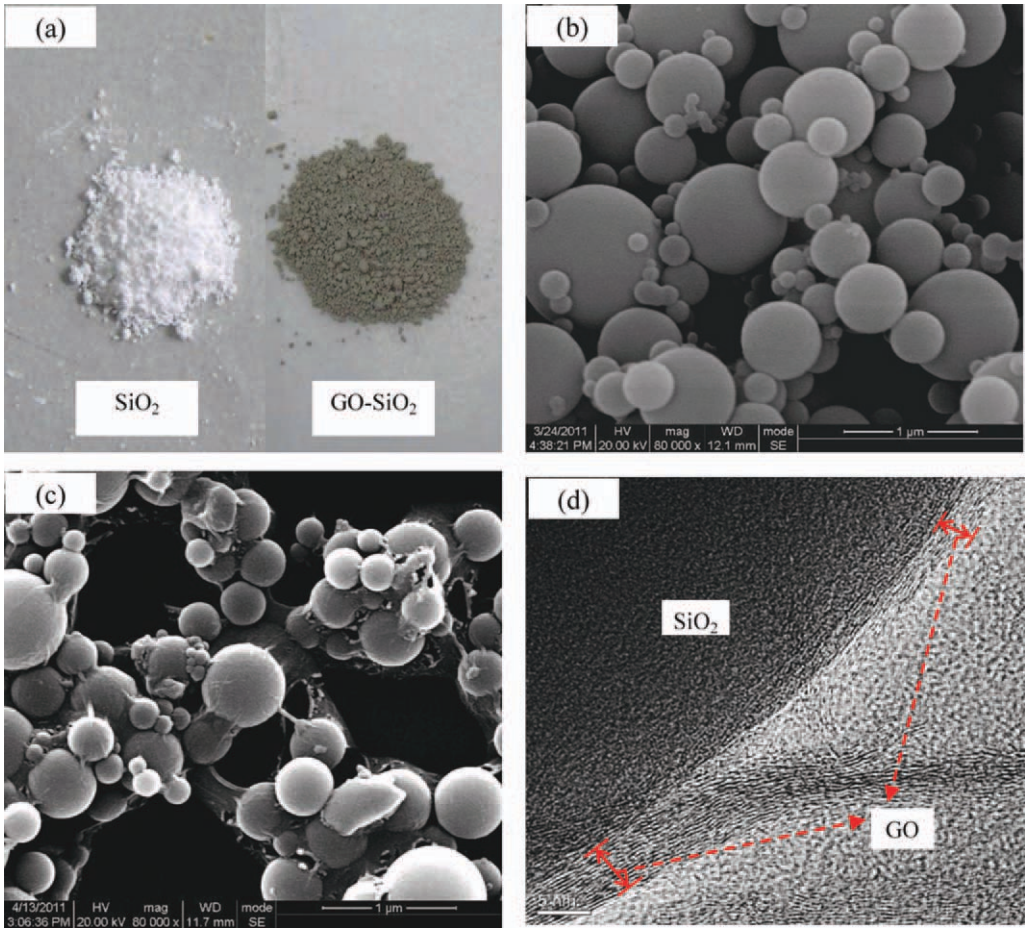

Figure 1 (a) Photographs of pristine SiO_2 and GO-SiO_2 hybrids; SEM images of (b) pristine SiO_2 and (c) GO-SiO_2 hybrids; (d) TEM images of GO-SiO_2 hybrids, showing core-shell structure with ultrathin GO sheets (<5 nm). [Color figure can be viewed in the online issue, which is available at wileyonlinelibrary.com.]

polypropylene pellets with the hybrids. The macroscopical dispersion can be conveniently observed by optical microscopy. Figure 2 shows the optical microscopy (OM) images of the pristine SiO_2 and GO-SiO_2 hybrids (10 wt %) dispersed in the maleated polypropylene. On the basis of the submicrometer size of SiO_2 and the properties of matrix, SiO_2 particles with some aggregations are observed in the matrix. Meanwhile, the GO-SiO_2 hybrids are well dispersed in the PP-*g*-MA as uniform black spots. It indicates that the compatibility between SiO_2 and maleated polypropylene is improved by introducing well-functional GO shell. Moreover, microcosmic dispersion and interface analysis will be discussed in the following SEM observation.

Interfacial interaction of core-shell structured GO-SiO_2 hybrids in maleated polypropylene composites

The interfacial interaction between filler and polymer is a vital factor to obtain high performance polymer composites. Switching the surface feature of filler is a popular way to enhance interfacial interaction. Thus, the interfacial interaction between the GO-SiO_2 hybrids and PP-*g*-MA should be systematically investigated.

Figure 3 shows the SEM images of fractured microstructure of PP-*g*-MA/SiO_2 and PP-*g*-MA/GO-SiO_2 composites with 10 wt % filler. Before SEM investigation, the injection molding samples were cryo-fractured in liquid nitrogen, perpendicularly to the flow direction. For the composites filled with SiO_2, many holes caused by pulled-out SiO_2 particles are visible and a few SiO_2 particles with smooth surfaces left in the fracture surface [Fig. 3(a,b)]. However, stronger interfaces are observed in fracture surfaces of composites filled with GO-SiO_2 hybrids. The hybrid particles show a well dispersion and tight coalescent in the matrix. The coated resin on the GO-SiO_2 hybrid can be clearly observed in the high magnification image as shown in Figure 3(d), indicating a strong interfacial interaction between GO-SiO_2 hybrids and PP-*g*-MA matrix.

To further compare the interfacial interaction of SiO_2 with PP-*g*-MA and GO-SiO_2 hybrids with PP-*g*-

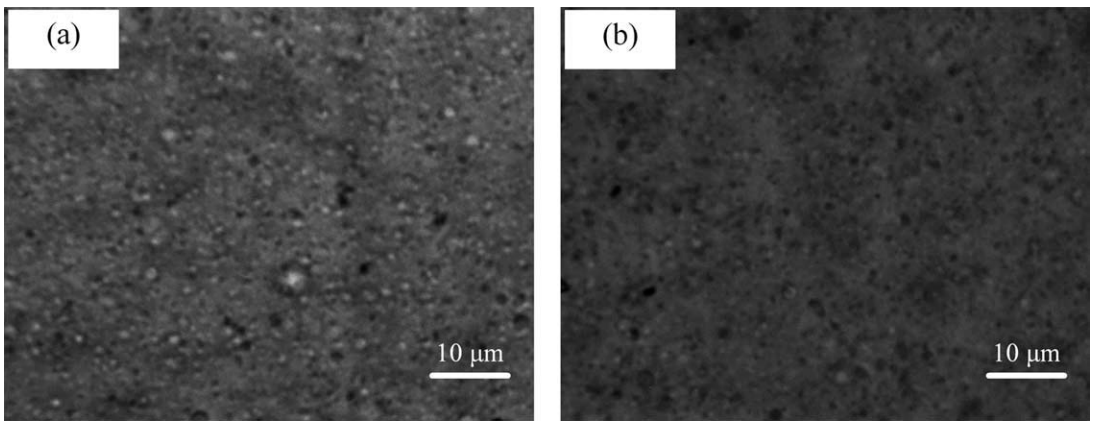

Figure 2 Optical micrographs showing the dispersion of fillers (10 wt %) in the PP-*g*-MA matrix: (a) the composite contains the pristine SiO_2 and (b) the composite contains the core-shell structured GO-SiO_2 hybrids.

MA, both of the composites were extracted in boiling xylene for 4 h by Soxhlet extraction technique. The extracted fillers were characterized by FTIR and TGA. Figure 4 shows the FTIR spectra of the pristine SiO_2, Ex-SiO_2, and Ex-GO-SiO_2 fillers. Because of the natural strong absorbency of SiO_2, the typical absorbant peaks of SiO_2 are shown in three kinds of fillers. Typically, the peaks at 1120 cm^{-1} and 805 cm^{-1} are ascribed to the asymmetric and symmetric stretching vibration of Si—O—Si.[35] Compared with pristine SiO_2, Ex-SiO_2, and Ex-GO-SiO_2 fillers shows two new peaks at 1462 cm^{-1} and 1380 cm^{-1}, which can be ascribed to the bending vibrations of —CH_2— (or —CH_3 asymmetric bending vibrations) and the

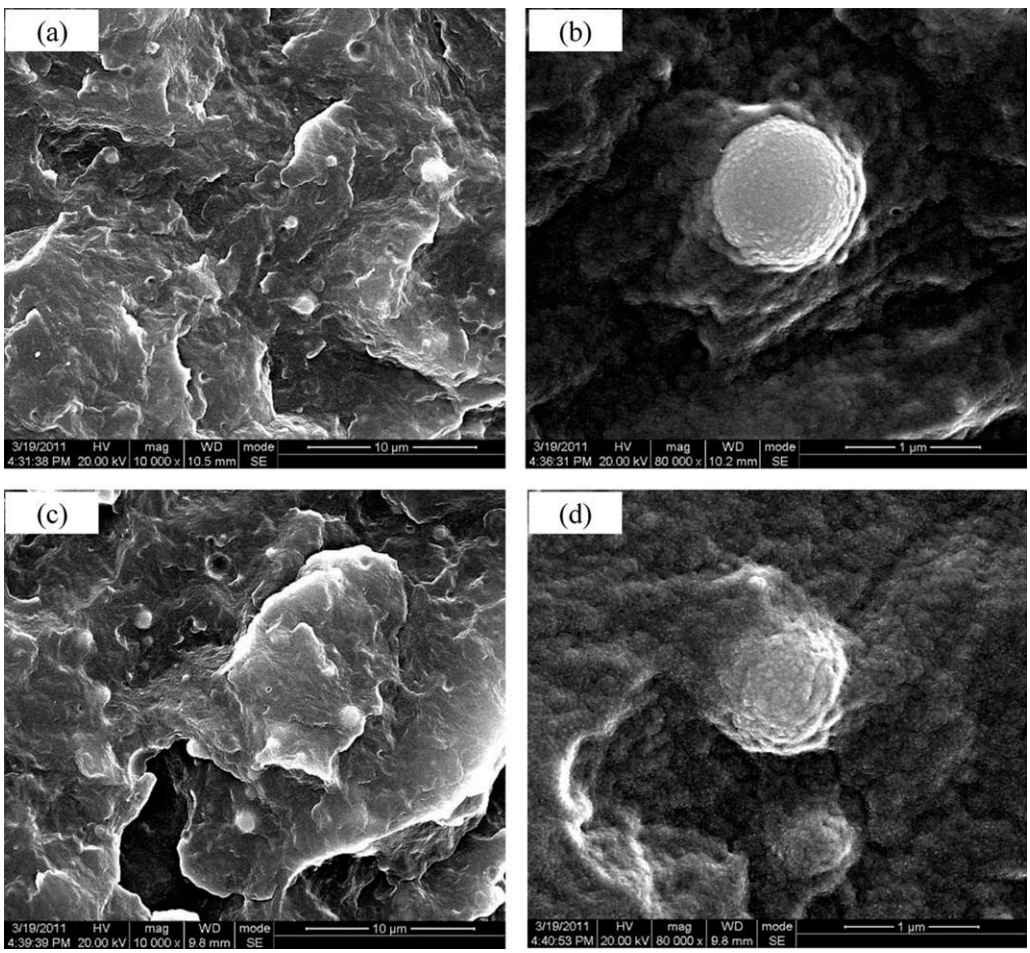

Figure 3 SEM images of fractured microstructure of (a,b) PP-*g*-MA/SiO_2 and (c,d) PP-*g*-MA/GO-SiO_2 composites with 10 wt % fillers.

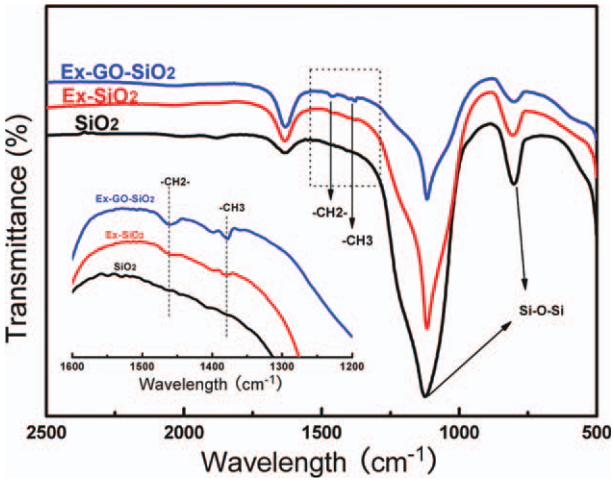

Figure 4 FTIR spectra of the SiO_2, Ex-SiO_2, and Ex-GO-SiO_2 fillers. The inset picture is magnified images for the peak belonging to bending vibration of —CH_2— and —CH_3 groups, respectively. [Color figure can be viewed in the online issue, which is available at wileyonlinelibrary.com.]

symmetric bending vibrations of —CH_3, respectively.[36] It indicates that matrix resin is still combined with the extracted fillers. Furthermore, the intensity of the two new peaks of Ex-GO-SiO_2 fillers is obviously stronger than that of Ex-SiO_2 (the inset picture of Fig. 4), implying more resin clinged to the extracted hybrids surface. There are two points that should be noticed. One is that the silane coupling agent of APS also has —CH_2— groups. It should be further discussed combining with the following TGA experiment to clarify where the —CH_2— groups might mainly come from. The other is that it is hard to identify the peak at about 1720 cm^{-1} related to the C=O vibration of carboxylic groups, which may be contributed to the functional groups of GO sheets and the maleic anhydride. It is possible that the

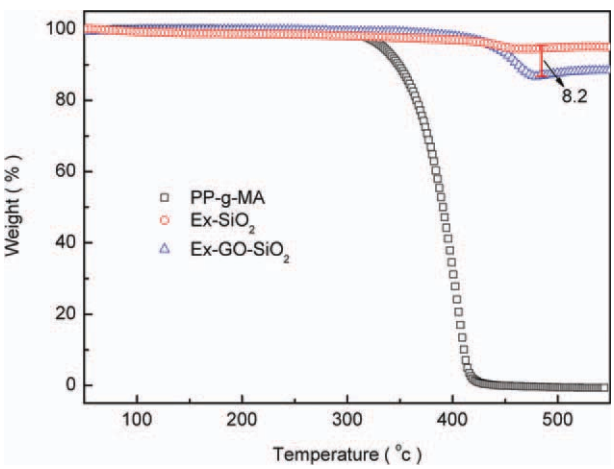

Figure 5 The weight loss curves for the neat PP-*g*-MA, Ex-SiO_2, and Ex-GO-SiO_2. [Color figure can be viewed in the online issue, which is available at wileyonlinelibrary.com.]

absorbency of Si—O—Si is much stronger than the absorbency of carboxylic groups and the content of GO sheets and maleic anhydride is quite less compared with the content of SiO_2. To further estimate the amount of matrix reserved on the fillers, thermogravimetric analysis (TGA) measurements were used. The weight loss curves of the neat PP-*g*-MA, Ex-SiO_2 and Ex-GO-SiO_2 are presented in Figure 5 and the corresponding data is listed in Table I. It is found that the main weight loss of neat PP-*g*-MA takes place in a temperature range between 300 and 450°C and 100 wt % weight loss of that takes place above 500°C. In contrast, the Ex-SiO_2 curve shows a little weight loss about 5.2% at temperature above 500°C, resulting from the quite little resin coated in the particle. While the Ex-GO-SiO2 curve shows more notable decrease at temperature above 450°C. From the weight loss of Ex-GO-SiO_2 around 500°C, the amount of the resin reserved on Ex-GO-SiO_2 particles is about 8.2 wt % higher than that of Ex-SiO_2 particles. As the TGA result proved, the weight of residual matrix is much more than the possible weight of APS (no more than 2 wt % of SiO_2). Therefore, we believe the two enhanced peaks at 1462 $cm^{-1}$and 1380 cm^{-1} mainly belong to the residual resin. In addition, it is easy to believe that the resin reserverd on the filler is the interphase, which can enhance the interfacial interaction between the filler and matrix. In other words, the interfacial thickness and interaction of PP-*g*-MA with GO-SiO_2 particles are better than that of PP-*g*-MA with SiO_2 particles. Generally, neat GO shows about 40% weight loss from 200 to 300°C in N_2 atmosphere.[37] However, in this work, the whole weight of GO coated on SiO_2 is only about 1 wt % (see Experimental section). As a result, the weight loss in this temperature range will be no more than 0.4 wt %. Therefore, the weight loss would be quite slight so that it can not be observed in this region. Moreover, compared with neat PP-*g*-MA, the onset temperature of weight loss of Ex-GO-SiO_2 (at 3 wt %) is significantly increased for 107.8°C. The effect of improved compatibility on enhanced thermal stability of matrix with GO has been widely reported in literature.[38,39] The result indicates that there is a strong interaction between the polymer matrix and the GO at the interface. Because of this, the mobility of the polymer

TABLE I
Thermo Gravimetric Analysis (TGA) Data of the Onset Temperature of Weight Loss (3%), Residual Weight, and Increased Temperature ($\Delta T_{(3\%)}$)

	$T_{onset\ (3\%)}$ (°C)	Residual weight (%)	$\Delta T_{(3\%)}$ (°C)
PP-*g*-MA	329.6	0	–
Ex-SiO_2	434.5	94.8	105.9
Ex-GO-SiO_2	437.4	86.6	107.8

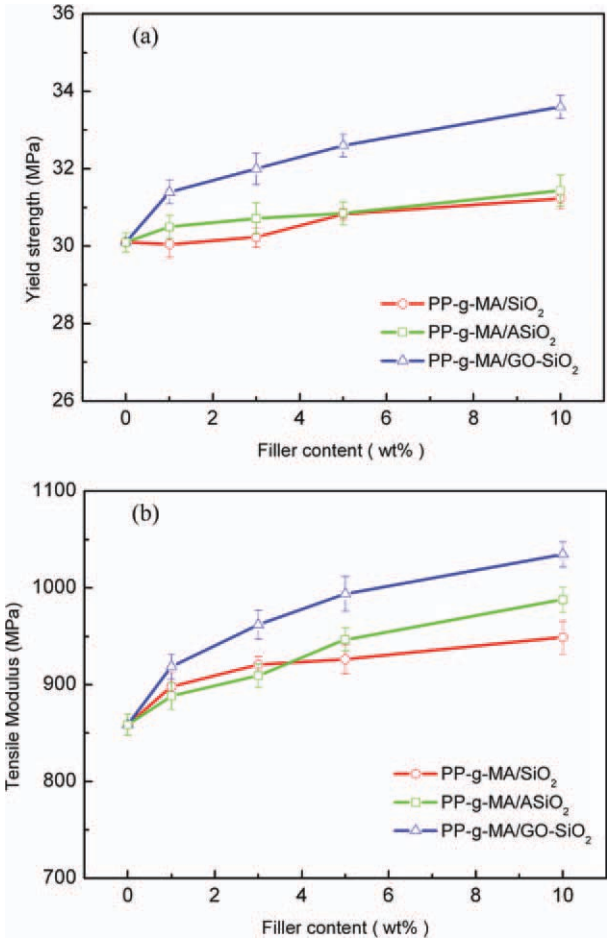

Figure 6 Effect of filler content on the (a) yield strength and (b) tensile modulus of PP-*g*-MA composites with SiO_2, amino-modified SiO_2 ($ASiO_2$), and GO-SiO_2 hybrids. [Color figure can be viewed in the online issue, which is available at wileyonlinelibrary.com.]

segments near the interface has become suppressed and introducing GO enhances the formation of char on the surface of polypropylene. As a consequence, it reduces the rate of decomposition. Combined with the ruselt of SEM, FTIR, and TGA, it is demonstrated that a thicker interphase and a stronger interaction were achieved by using this GO-SiO_2 hybrid particles filled PP-*g*-MA compared with pristine SiO_2 filled PP-*g*-MA.

Mechanical reinforcement of GO-SiO_2 hybrids in maleated polypropylene composites

The core-shell structured hybrid particles can hold great promise to reinforce polymer composites due to its large aspect ratio and strong interfacial interaction with matrix. The reinforcement effect of these hybrid particles is obvious for the tensile properties as illustrated in Figure 6. It is obvious that the improvement of mechanical properties of composites filled with GO-SiO_2 is stronger than that of composites filled with SiO_2 and amino-modified SiO_2. Comparing with the neat PP-*g*-MA, the yield strength increased from 30 to 33.6 MPa for composites containing 10 wt % GO-SiO_2 hybrids, while the yield strength only increase to 31.2 and 31.5 MPa for composites containing 10 wt % SiO_2 and amino-modified SiO_2 particles, respectively. More importantly, the tensile modulus of composites containing 10 wt % GO-SiO_2 hybrids is up to 1034 MPa compared with 948 MPa for composites containing 10 wt % SiO_2 and 805 MPa for neat PP-*g*-MA. Although the silane coupling agent with amino group might also have good interaction with PP-*g*-MA, the effective coupling group and contactile surface area of amino-modified SiO_2 are much less than that of GO-SiO_2. This might be the reason why there is a little effect of amino-modified SiO_2 particles on enhancing PP-*g*-MA. It is well known that the loads can be transferred from the matrix to the filler through an interfacial region. Therefore, the mechanical reinforcement of maleated polypropylene composites filled by GO-SiO_2 hybrids can be another proof of interfacial enhancement.

What is more, DMA measurement can be an effective method to estimate the interfacial interaction between the filler and matrix.[40,41] Especially, the storage modulus is much sensitive to the particle dispersion and interfacial interaction in matrix. Figure 7 shows the dynamic storage modulus (G') versus the temperature curves of PP-*g*-MA and its composites. The data of storage modulus values at -40, 20, and 60°C from the DMA results for neat PP-*g*-MA and its nanocomposites are summarized in Table II. On the whole, the storage modulus of filled PP-*g*-MA increases with addition of both types of fillers. It was found that the reinforcing effect of GO-SiO_2 hybrids is more prominent in PP-*g*-MA/

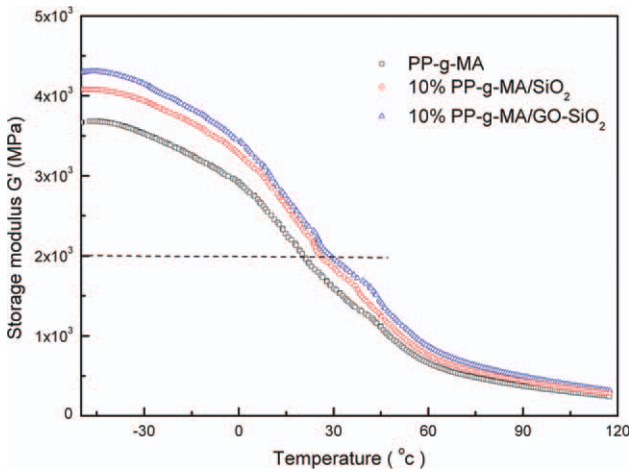

Figure 7 Storage modulus (G') versus temperature of PP-*g*-MA and its composites tested by DMA at a frequency of 1 Hz. [Color figure can be viewed in the online issue, which is available at wileyonlinelibrary.com.]

TABLE II
DMA Data of Storage Modulus (G') of PP-*g*-MA and Its Composites at Various Temperatures, and the Corresponding Temperatures When Storage Modulus Is at 2GPa

	G' (MPa, −40°C)	G' (MPa, 20°C)	G' (MPa, 60°C)	$T_{(2GPa)}$ (°C)
PP-*g*-MA	3658	2025	660	20.5
10% PP-*g*-MA/SiO_2	4050	2340	763	25.8
10% PP-*g*-MA/GO-SiO_2	4275	2470	867	29.1

GO-SiO_2 than PP-*g*-MA/SiO_2 at whole test temperature range. For example, the storage modulus of PP-*g*-MA composite containing 10 wt % GO-SiO_2 hybrids increases dramatically to 4275 MPa (at −40°C) in the glassy region, which is 17% larger than that (3658 MPa) of neat PP-*g*-MA as well as 6% larger than that (4050 MPa) of composite containing 10 wt % SiO_2 particles, indicating that the hybrids are homogeneously dispersed and have strong interfacial adhesion with the matrix. In addition, the curves of storage modulus (G') show a few degrees shift to high temperature with addition of fillers, indicating an increase of glass transition temperature and thus increase of interfacial interaction by adding fillers. This should be explained by the fact that the presence of hybrid fillers in the composite will increase the hindrance of the segmental motion of the PP-*g*-MA chains due to the effects of interfacial interaction. Typically, when storage modulus is at 2 GPa, the corresponding temperatures of neat PP-*g*-MA, 10% PP-*g*-MA/SiO_2 and 10% PP-*g*-MA/GO-SiO_2 are 20.5, 25.8, and 29.1°C, respectively.

The mechanisms of interfacial enhancement of GO-SiO_2 hybrids in maleated polypropylene composites and outlook

As mentioned above, the novel core-shell structure GO-SiO_2 hybrids shows enhanced interfacial interaction with maleated polypropylene. It is due to the ultrathin GO sheets with special large surface and well-functional groups as a flexible shell coated on SiO_2 to switch the surface feature of the filler. To understand the formation processes precisely, the scheme of overall fabricating procedure of self-assembly core-shell structured GO-SiO_2 hybrids and its polymer composites are plotted in Figure 8. The fabricate procedure of polymer/GO-SiO_2 composite involves three steps: SiO_2 particles were firstly modified by surface grafting of 3-aminopropyltriethoxysilane (APS) to render the SiO_2 surface positively charged. Meanwhile, the graphite was oxidized into negatively charged graphene oxide by Hummers method. Then, the amino-modified SiO_2 particles were assembled with graphene oxide to form core-shell structured GO-SiO_2 hybrids by electrostatic interaction. Finally, the resulting hybrids were added into polymer via melt blending resulting in polymer composite. Here, the interfacial enhancement of this hybrid composite is determined by not only the interaction between GO and modified SiO_2 but also the interaction between GO and the matrix. For the interaction between GO and modified SiO_2, It is thought that the epoxide groups in the GO sheets react with the amino groups on the modified SiO_2 particle surface via a ring-opening reaction,[23,42] as well as the amido linkage between carboxylic and

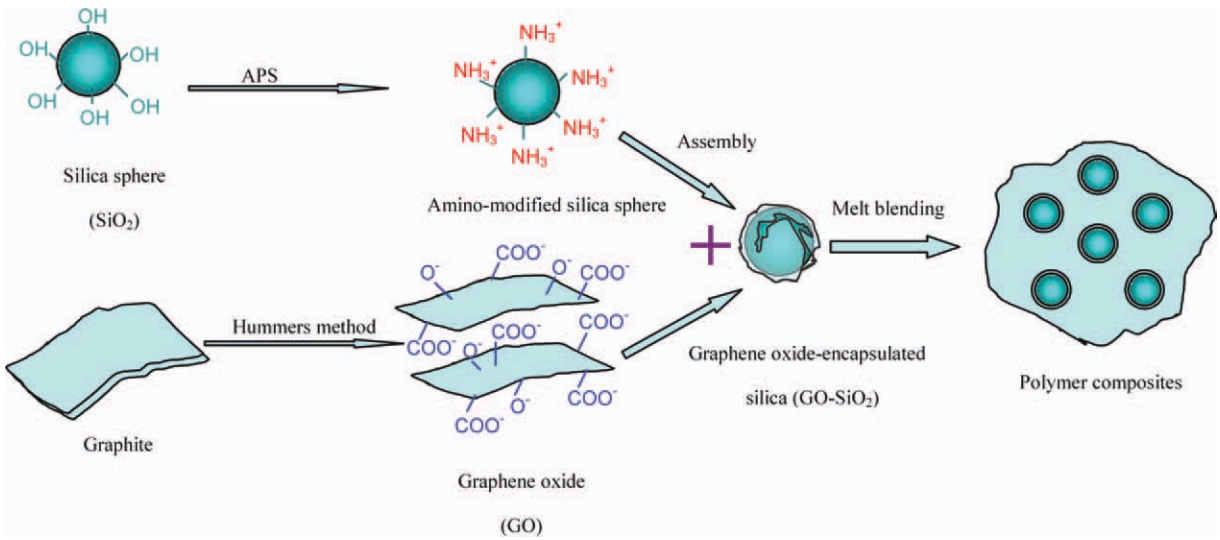

Figure 8 The scheme of overall fabricating procedure of self-assembly core-shell structured GO-SiO_2 hybrids and its polymer composites, including (1) modification of SiO_2 by grafting 3-aminopropyltrimethoxysilane (APS) and preparation of graphene oxide (GO) sheets by Hummers method, (2) hybrid assembly between positively charged amino-modified SiO_2 and negatively charged GO by electrostatic interactions, and (3) melt blending. [Color figure can be viewed in the online issue, which is available at wileyonlinelibrary.com.]

amino groups is supposed to be formed during thermal processing.[43,44] Thus, the GO sheets and SiO_2 particles bond together by forming covalent chemical bonds to form a robust core-shell structure. On the other hand, graphene oxide (GO) contains abundant oxygenous groups both on the basal planes and at the edges of graphene oxide sheets[17,18,45]; thus, it is logical to obtained good compatibility between PP-*g*-MA and GO-SiO_2 hybrids due to the similar polarity and possible H-bonding of polar groups between PP-*g*-MA and GO.[14,41] Therefore, the strong interfacial interaction and improved mechanical properties of PP-*g*-MA/GO-SiO_2 composites can be achieved.

Furthermore, the ultrathin graphene Oxide shells of this hybrid can be reduced into graphene through chemical or thermal reduction.[7,15,46,47] These reduced graphene Oxide-based hybrid particles can be a great diversity of technological applications including nanoelectronic and photoelectronic components,[19,48] energy storage materials,[49] polymer composites,[16,47,50] electrocatalysis,[51] etc. The novel hybrids also provide a useful way to disperse and design architectural graphene.[17,21,31] Moreover, maleated polypropylene has long been used as compatibilizer in commercial blend and composites. These hybrids filled maleated polypropylene composite can be further blend with other polymers to achieve special functionalization and performance.

CONCLUSIONS

In summary, a novel core-shell structured hybrid particle was coassembled by ultrathin negatively charged graphene oxide sheets and positively charged amino-modified silica through a simple solution mixing. SEM, OM, FTIR, TGA, and DMA demonstrated that this hybrid shows a good dispersion and enhanced interfacial interaction with PP-*g*-MA, thus leading to improved mechanical performance. We believe that this work will provide a potential application of graphene oxide-encapsulated particle to achieve special performance.

References

1. Rao, C. N. R.; Sood, A. K.; Subrahmanyam, K. S.; Govindaraj, A. Angew Chem Int Ed 2009, 48, 7752.
2. Geim, A. K.; Novoselov, K. S. Nat Mater 2007, 6, 183.
3. Lee, C.; Wei, X.; Kysar, J. W.; Hone, J. Science 2008, 321, 385.
4. Du, X.; Skachko, I.; Barker, A.; Andrei, E. Y. Nat Nanotechnol 2008, 3, 491.
5. Balandin, A. A.; Ghosh, S.; Bao, W.; Calizo, I.; Teweldebrhan, D.; Miao, F.; Lau, C. N. Nano Lett 2008, 8, 902.
6. Bolotin, K. I.; Sikes, K. J.; Jiang, Z.; Klima, M.; Fudenberg, G.; Hone, J.; Kim, P.; Stormer, H. L. Solid State Commun 2008, 146, 351.
7. Schniepp, H. C.; Li, J. L.; McAllister, M. J.; Sai, H.; Herrera-Alonso, M.; Adamson, D. H.; Prud'homme, R. K.; Car, R.; Saville, D. A.; Aksay, I. A. J Phys Chem B 2006, 110, 8535.
8. Novoselov, K. S.; Geim, A. K.; Morozov, S. V.; Jiang, D.; Zhang, Y.; Dubonos, S. V.; Grigorieva, I. V.; Firsov, A. A. Science 2004, 306, 666.
9. Kim, K. S.; Zhao, Y.; Jang, H.; Lee, S. Y.; Kim, J. M.; Kim, K. S.; Ahn, J. H.; Kim, P.; Choi, J. Y.; Hong, B. H. Nature 2009, 457, 706.
10. Rollings, E.; Gweon, G. H.; Zhou, S. Y.; Mun, B. S.; McChesney, J. L.; Hussain, B. S.; Fedorov, A. V. J Phys Chem Solids 2006, 67, 2172.
11. De Heer, W. A.; Berger, C.; Wu, X. Solid State Commun 2007, 143, 92.
12. Park, S.; Ruoff, R. S. Nat Nanotechnol 2009, 4, 217.
13. Yang, X.; Dou, X.; Rouhanipour, A.; Zhi, L.; R der, H. J.; Müllen, K. J Am Chem Soc 2008, 130, 4216.
14. Dikin, D. A.; Stankovich, S.; Zimney, E. J.; Piner, R. D.; Dommett, G. H. B.; Evmenenko, G.; Nguyen, S. B. T.; Ruoff, R. S. Nature 2007, 448, 457.
15. Stankovich, S.; Dikin, D. A.; Piner, R. D.; Kohlhaas, K. A.; Kleinhammes, A.; Jia, Y.; Wu, Y.; Nguyen, S. B. T.; Ruoff, R. S. Carbon 2007, 45, 1558.
16. Ramanathan, T.; Abdala, A. A.; Stankovich, S.; Dikin, D. A.; Herrera-Alonso, M.; Piner, R. D.; Adamson, D. H.; Schniepp, H. C.; Chen, X.; Ruoff, R. S. Nat Nanotechnol 2008, 3, 327.
17. Kim, F.; Cote, L. J.; Huang, J. Adv Mater 2010, 22, 1954.
18. Lerf, A.; He, H.; Forster, M.; Klinowski, J. J Phys Chem B 1998, 102, 4477.
19. Yang, S.; Feng, X.; Ivanovici, S.; Müllen, K. Angew Chem Int Ed 2010, 49, 8408.
20. Han, T. H.; Lee, W. J.; Lee, D. H.; Kim, J. E.; Choi, E. Y.; Kim, S. O. Adv Mater 2010, 22, 2060.
21. Luechinger, N. A.; Booth, N.; Heness, G.; Bandyopadhyay, S.; Grass, R. N.; Stark, W. J. Adv Mater 2008, 20, 3044.
22. Hong, J.; Char, K.; Kim, B. S. J Phys Chem Lett 2010, 1, 3442.
23. Oh, J.; Lee, J. H.; Koo, J. C.; Choi, H. R.; Lee, Y.; Kim, T.; Luong, N. D.; Nam, J. D. J Mater Chem 2010, 20, 9200.
24. Goncalves, G.; Marques, P. A. A. P.; Granadeiro, C. M.; Nogueira, H. I. S.; Singh, M. K.; Gracio, J. Chem Mater 2009, 21, 4796.
25. Lightcap, I. V.; Kosel, T. H.; Kamat, P. V. Nano Lett 2010, 10, 577.
26. Si, Y.; Samulski, E. T. Chem Mater 2008, 20, 6792.
27. Williams, G.; Kamat, P. V. Langmuir 2009, 25, 13869.
28. Williams, G.; Seger, B.; Kamat, P. V. ACS Nano 2008, 2, 1487.
29. Zou, H.; Wu, S.; Shen, J. Chem Rev 2008, 108, 3893.
30. Hummers Jr, W. S.; Offeman, R. E. J Am Chem Soc 1958, 80, 1339.
31. Cote, L. J.; Kim, F.; Huang, J. J Am Chem Soc 2008, 131, 1043.
32. Kim, J.; Cote, L. J.; Kim, F.; Yuan, W.; Shull, K. R.; Huang, J. J Am Chem Soc 2010, 132, 8180.
33. Vickery, J. L.; Patil, A. J.; Mann, S. Adv Mater 2009, 21, 2180.
34. Li, D.; Muller, M. B.; Gilje, S.; Kaner, R. B.; Wallace, G. G. Nat Nanotechnol 2008, 3, 101.
35. Almeida, R. M.; Guiton, T. A.; Pantano, C. G. J Non-Cryst Solids 1990, 121, 193.
36. Chen, X.; Yu, J.; Luo, Z.; Hu, S.; Zhou, Z.; Guo, S.; Lu, S. J Polym Res 2009, 16, 745.
37. Kou, L.; Gao, C. Nanoscale 2011, 3, 519.
38. Cao, Y.; Feng, J.; Wu, P. Carbon 2010, 48, 1683.
39. Liu, N.; Luo, F.; Wu, H.; Liu, Y.; Zhang, C.; Chen, J. Adv Funct Mater 2008, 18, 1518.
40. Zhou, T. H.; Ruan, W. H.; Mai, Y. L.; Rong, M. Z.; Zhang, M. Q. Compos Sci Technol 2008, 68, 2858.
41. Cerezo, F. T.; Preston, C. M. L.; Shanks, R. A. Macromol Mater Eng 2007, 292, 155.

42. Park, S.; Dikin, D. A.; Nguyen, S. B. T.; Ruoff, R. S. J Phys Chem C 2009, 113, 15801.
43. Mo, Y.; Zhu, M.; Bai, M. Colloid Surface A 2008, 322, 170.
44. Ou, J.; Wang, J.; Liu, S.; Mu, B.; Ren, J.; Wang, H.; Yang, S. Langmuir 2010, 26, 15830.
45. Cai, W.; Piner, R. D.; Stadermann, F. J.; Park, S.; Shaibat, M. A.; Ishii, Y.; Yang, D.; Velamakanni, A.; An, S. J.; Stoller, M. Science 2008, 321, 1815.
46. Kang, H.; Kulkarni, A.; Stankovich, S.; Ruoff, R. S.; Baik, S. Carbon 2009, 47, 1520.
47. Stankovich, S.; Dikin, D. A.; Dommett, G. H. B.; Kohlhaas, K. M.; Zimney, E. J.; Stach, E. A.; Piner, R. D.; Nguyen, S. B. T.; Ruoff, R. S. Nature 2006, 442, 282.
48. Gilje, S.; Han, S.; Wang, M.; Wang, K. L.; Kaner, R. B. Nano Lett 2007, 7, 3394.
49. Stoller, M. D.; Park, S.; Zhu, Y.; An, J.; Ruoff, R. S. Nano Lett 2008, 8, 3498.
50. Xu, Y.; Hong, W.; Bai, H.; Li, C.; Shi, G. Carbon 2009, 47, 3538.
51. Tang, L.; Wang, Y.; Li, Y.; Feng, H.; Lu, J.; Li, J. Adv Funct Mater 2009, 19, 2782.